

Computer Simulation of Phase Structure and Mechanical Properties of Polymer Mixtures

TAKAAKI MATSUOKA, SATORU YAMAMOTO

Toyota Central Research and Development Laboratories, Inc., 41-1, Aza Yokomichi, Oaza Nagakute, Nagakute-Cho, Aichi-Gun, Aichi-Ken, 480-1192, Japan

Received 18 September 1997; accepted 27 October 1997

ABSTRACT: Computer programs have been developed to predict phase separation, flow-induced phase structure, and structure-dependent mechanical properties of binary polymer mixtures. The phase separation is simulated by solving a two-dimensional Langevin equation with Flory–Huggins free energy using the finite difference method under periodic boundary conditions. The change of phase structure due to flow is predicted by adding a shear flow term to the equation. By generating a finite element mesh from the calculated phase structure, the stress analysis is carried out for estimating the mechanical properties of the system using the finite element method. The elastic modulus and thermal expansion coefficient based on the phase structure were numerically investigated for various volume fractions and properties of components using the developed programs. © 1998 John Wiley & Sons, Inc. *J Appl Polym Sci* 68: 807–813, 1998

Key words: computer simulation; phase separation; morphology; finite element method; elastic modulus; thermal expansion coefficient

INTRODUCTION

The characteristics of polymer mixtures, such as polymer alloys and blends, have been investigated to develop materials with superior properties. Almost all commercially important polymer alloys and blends exhibit phase separation and have their own fine structures. The morphology has an influence on their properties. Many theoretical and empirical models were proposed for estimating the properties of mixtures. Several models were summarized for the elastic modulus¹ and the thermal expansion coefficient.² A model for the prediction of the elastic response over a wide range of concentration was presented for spherical particulate composites by Farber and Farris.³ Predictive models based on micromechanics were studied for particulate composites.^{4,5} Guild and

Young applied a finite element analysis to study a predictive model for particulate-filled materials.⁶ The usage of these models are, however, restricted within narrow limits because it is difficult to consider the change of the structure, size, and shape of the droplets. An understanding of the relation between properties and structures is still lacking because of structural complexity.

The phase separation is phenomenologically described by the Cahn–Hilliard–Cook model,^{7,8} which is a diffusion equation for spinodal decomposition. This equation was numerically solved and used for the investigation of phase separation by Petschek and Metiu,⁹ Chakrabarti et al.,¹⁰ Ariyapadi et al.,¹¹ and Chen et al.¹² These previous studies indicate that the Cahn–Hilliard–Cook equation can be used for the prediction of phase separation in binary polymer systems.

The aim of our study was the development of computer programs for predicting the phase structures and mechanical properties of binary polymer mixtures and the numerical investiga-

Correspondence to: T. Matsuoka.

tion of the relationship between the structures and properties. The phase structure due to phase separation was simulated in the previous article.¹³ The effect of polymer properties, which are the degree of polymerization, segment length, and solubility parameter, on the phase separation and structure was numerically investigated there. In this article, moreover, the change of the phase structure owing to shear flow was computed. Then, the mechanical properties, elastic modulus, and thermal expansion coefficient were predicted from the computed structures by a stress analysis using the finite element method.

THEORY

The phase separation of binary polymer mixtures is described in dimensionless form by the following equation, which is derived from the nonlinear Langevin equation and Flory-Huggins free energy:

$$\partial\phi/\partial t = (\frac{1}{2})\nabla^2(-\phi + \phi^3 - \nabla^2\phi) - \nabla u \phi \quad (1)$$

where ϕ is the order parameter related to the volume fraction of one of the polymers; t , the time; and u , the velocity. The last term of the equation means the effect of flow on the phase structure. Here, we consider a simple shear flow:

$$u = (\dot{\gamma}y, 0, 0) \quad (2)$$

$\dot{\gamma}$ is the shear rate in the x - y - z rectangular coordinates.

The elastic modulus E of binary mixtures is simply described by the following models:

Parallel model:

$$E_m = E_1f_1 + E_2f_2 \quad (3)$$

Series model:

$$E_m = E_1E_2/(E_1f_2 + E_2f_1) \quad (4)$$

where f is the volume fraction of the component and subscripts m , 1, and 2 denote the mixture and components 1 and 2, respectively.

For the thermal expansion coefficient α , the models become as follows:

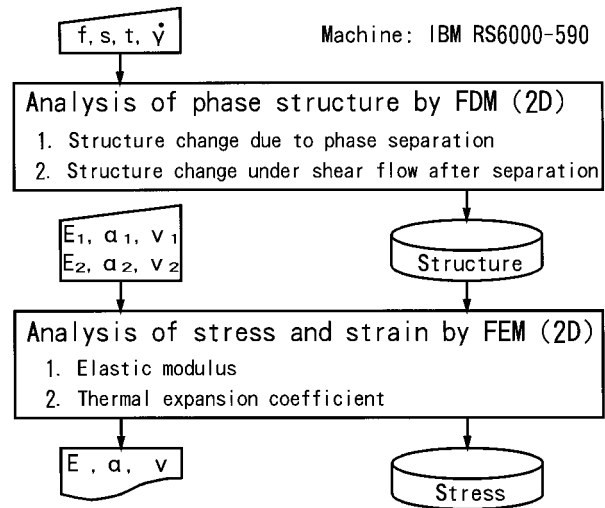


Figure 1 Flow chart for computation.

Parallel model:

$$\alpha_m = (\alpha_1E_1f_1 + \alpha_2E_2f_2)/(E_1f_1 + E_2f_2) \quad (5)$$

Series model:

$$\alpha_m = \alpha_1f_1 + \alpha_2f_2 \quad (6)$$

The parallel model for E and the series model for α are also called the additive rule.

These models are usually considered as upper and lower bounds. There are other models which more closely describe practical observations of particle-dispersed systems, for example, the Hirsh model, Takayanagi model, and Counto model for the elastic modulus and the Kerner model, Turner model, and Schapery model for thermal expansion. However, we should select a model according to the shape and properties of the particles in actual usage. In this article, the parallel model and series model were used for the discussion on the calculated results.

CALCULATION

The flow chart for computation is shown in Figure 1. Two kinds of main analysis programs have been developed in two-dimensional space. One is an analysis program of phase separation using the finite difference method (FDM). The other is a stress analysis program using the finite element method (FEM). At the beginning, the analysis of phase structure is carried out. The previous

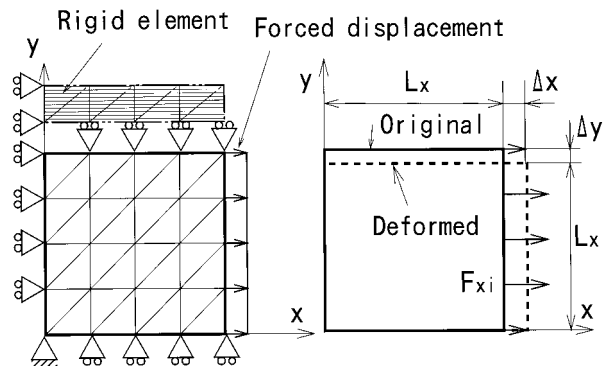


Figure 2 Finite element mesh and boundary conditions for predicting the elastic modulus.

equation for phase separation is solved for simulating the structure change due to phase separation and shear flow. Input data are the volume fraction, the size of analysis grid, the time, and the shear rate. Then, the calculated results of structures are output in a data file for the following analysis. Next, the stress analysis is performed for the calculated structures by the FEM. The macroscopic elastic modulus and thermal expansion coefficient of the mixture system are estimated from the results of the stress analysis and the mechanical properties of two polymer components.

Figure 2 shows a finite element mesh and boundary conditions for predicting the elastic modulus, and Figure 3, for the thermal expansion coefficient. Triangular plane stress elements are used for the analysis. Boundary conditions are defined to keep a rectangular shape of the region. In other words, the upper side is parallel to the lower side, and the right side is parallel to the left side for any given time. To achieve these conditions, two rigid bodies, of which the elastic moduli are large enough to prevent their deformation, are

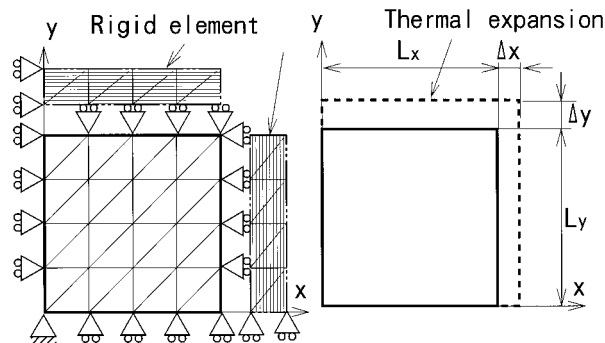


Figure 3 Finite element mesh and boundary conditions for predicting the thermal expansion coefficient.

Table I Calculation Conditions

For computing phase structures	
Lattice grid	128 × 128
Initial state	Miscible
Boundary	Periodic
Fraction of polymer 2	0.1–0.9
Phase separation time	200
Shear rate	1
Shear strain	2
For predicting mechanical properties	
Elastic modulus	$E_1/E_2 = 1/10, 10/1$
Thermal expansion coefficient	$\alpha_1/\alpha_2 = 10/1$
Poisson's ratio	$\nu_1 = \nu_2 = 0.4$
Boundary	Parallel

virtually introduced out of the region and along the upper and right sides. Then, it is set that the nodes on the upper and right sides can only slide on the surface of the neighbor rigid body. The y -directional displacement of the nodes located on the x axis and the x -displacement of ones on the y axis are constrained. In actual calculation, the finer mesh and necessary boundary conditions are automatically generated from each phase structure. By giving a forced displacement for E and a temperature change for α , the region will be deformed like the broken line shape. The elastic moduli in the x and y directions, E_x and E_y , are estimated from the summation of the nodal forces F_x and F_y using the following equations, respectively:

$$E_x = \sum F_{xi} L_x / (\Delta x L_y) \tag{7}$$

$$E_y = \sum F_{yi} L_y / (\Delta y L_x) \tag{8}$$

The thermal expansion coefficients, α_x and α_y , are calculated from the nodal displacements Δx and Δy , respectively:

$$\alpha_x = \Delta x / (L_x \Delta T) \tag{9}$$

$$\alpha_y = \Delta y / (L_y \Delta T) \tag{10}$$

Calculation conditions are summarized in Table I. A lattice grid of 128 × 128 was used for computing the phase structures. It was assumed that two polymers are in a miscible region at the initial time and then quenched in an immiscible region. As the thermal noise term is neglected,

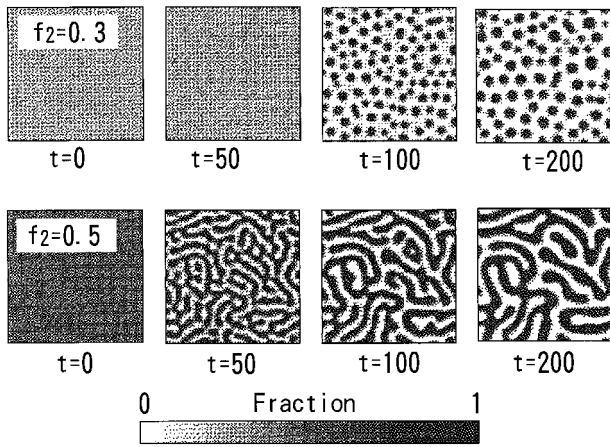


Figure 4 Computed phase structure during phase separation.

and to start the phase separation, the initial fractions were chosen to be randomly distributed between -0.01 and 0.01 about the average fraction as the initial condition. The periodic boundary condition is used to consider an infinite domain. The average fraction of polymer 2 is varied from 0.1 to 0.9 in an interval of 0.1 . Computer runs were performed out to a nondimensional time of 200 , at which the phase separation will be in the late stage of the decomposition and be almost completed. After phase separation, a shear flow of a shear rate of 1 was applied to the separated structures for a time of 2 , namely, the shear strain becomes 2 . For predicting mechanical properties, two cases of calculations were carried out for the elastic modulus. Elastic moduli of components 1 and 2 are 1 over 10 and 10 over 1 , while the ratio of thermal expansion coefficients are 10 over 1 and both Poisson's ratios are 0.4 . The boundaries of the region are parallel.

RESULTS

Phase Structures

Computed phase structures during phase separation are shown in Figure 4 for volume fractions 0.3 and 0.5 . At the initial time, the fractions are unique about each average fraction. For fraction 0.3 , a little fluctuation appears at time 50 , and this fluctuation grows up to the droplet and matrix-type structures at time 100 . After that, the droplets become larger because of coarsening. For fraction 0.5 , the phase separation is already observed at time 50 and it begins at an earlier time

than that of fraction 0.3 . The separated structure is different from that of fraction 0.3 and is called a percolated type, and it is coarsening as it is with time. Calculated results are verified by comparing them with experimental ones on the time evolution of the wavenumber during phase separation in the previous article.¹³

Figure 5 shows phase structures calculated for various average fractions at a time of 200 . When the average fraction is 0.2 and less, or 0.8 and more, the phase separation does not occur; therefore, these fractions are in the miscible region. For the average fractions of 0.3 and 0.4 , the morphology becomes a droplet and matrix structure, in which the droplet is polymer 2 . When the fraction is 0.4 , droplets are greater than those in fraction 0.3 , and some conjunctions of droplets are observed. If the fraction is 0.5 , the structure shows a percolated type because the system is symmetric. For the fractions of 0.6 and 0.7 , the structures become droplet and matrix ones again; however, the droplet is polymer 1 .

A simple shear flow was applied to the calculated structures caused by phase separation. The structures deformed by shear flow are shown in Figure 6. The flow is caused by moving the upper side left to right. The miscible phases for fractions 0.2 and 0.8 have no change. The droplets are extended and deformed in the flow direction. The percolated structure is also extended to the flow direction as it still remains the percolated state. Since the structural orientation is clear, macroscopic properties in the flow direction are easily expected to be different from those in its transverse direction.

These results are calculated in a nondimen-

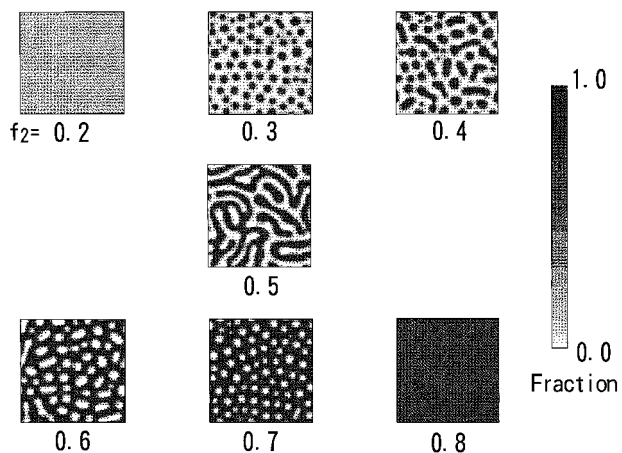


Figure 5 Phase structures calculated for various average fractions at a time of 200 .

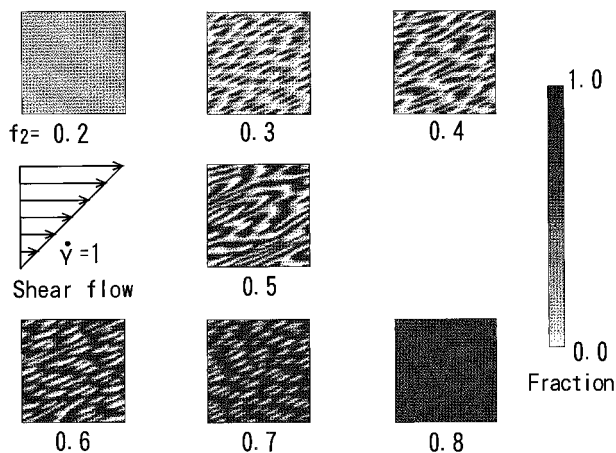


Figure 6 Phase structures deformed by shear flow.

sional scale. Therefore, to apply the simulation to actual polymer alloys and blends, the calculation should be carried out in a real scale. The relation between a nondimensional scale and a real scale was discussed in our previous work.¹³ For example, when the difference between solubility parameters is small, the calculation demonstrates that the interface between compositions becomes vague in a real scale. In this case, the region where the percolated structure is found will be much wider than the single 50/50 composition range in practice.

Mechanical Properties

The computed relative elastic moduli of mixtures with separated structures are plotted against the volume fraction as shown in Figure 7. The relative elastic modulus is defined as a ratio of the pre-

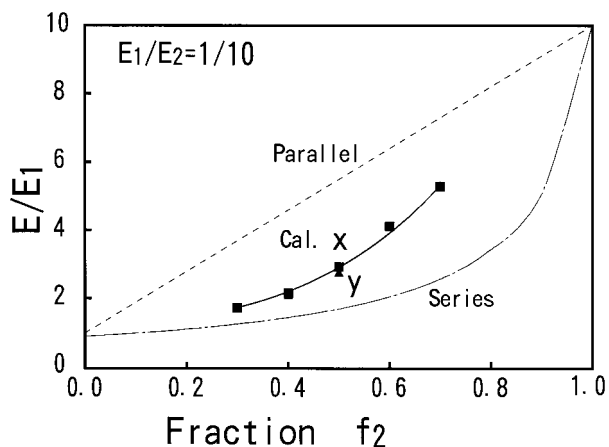


Figure 7 Predicted elastic modulus against volume fraction.

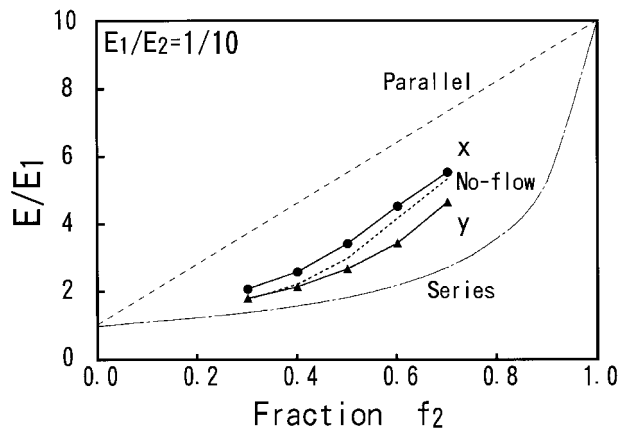


Figure 8 Effect of the shear flow on the relative elastic modulus.

dicted elastic modulus to that of polymer 1. The broken line indicates the parallel model, which is the same as the additive rule of mixing, and the dash-dotted curve denotes the series model. The predicted results are just between both models. As the difference between the *x* and *y* results is small, it can say that the mixture is still isotropic on the elastic modulus after phase separation.

Figure 8 shows the effect of the shear flow on the relative elastic modulus. The dotted curve labeled with no-flow is the same result as the *x*-elastic modulus shown in the previous plot and shows the initial property before flow. By applying the shear flow, the elastic modulus increases from the initial one in the *x* or flow direction, but decreases in the *y* direction. It was predicted that the anisotropy of the elastic modulus is caused by the flow.

The predicted relative thermal expansion coefficients, which are evaluated against that of polymer 2, are shown in Figure 9. The broken line indicates the series model or the additive rule and two dash-dotted curves denote the parallel model. The parallel model is indicated with the upper curve when $E_1 > E_2$ and with the lower one when $E_1 < E_2$. If E_1 is equal to E_2 , it is the same as the series model. The predicted results demonstrate that the relative thermal expansion coefficients increase from the series model when $E_1/E_2 = 10/1$, but decrease when $E_1/E_2 = 1/10$ as the parallel model suggests. The elastic modulus has a large effect on the thermal expansion. The *x* and *y* results are almost similar in each case, so it was said that the anisotropy of the mechanical properties is not caused by phase separation only.

Figure 10 shows the effect of the shear flow on the thermal expansion coefficient. For $E_1 < E_2$,

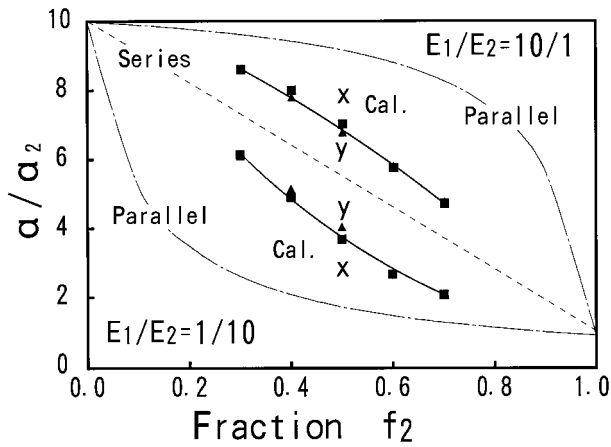


Figure 9 Predicted relative thermal expansion coefficients versus volume fraction.

the thermal expansion coefficient increases in the x direction with flow and decreases in the y direction. Inversely, in the case of $E_1 > E_2$, it decreases in the x direction and increases in the y direction. The opposite tendency is due to the elastic modulus. This was considered as follows: As shown in the phase structure change due to flow, the droplets are deformed and laminated along the x direction by shear flow. The structure becomes similar to a parallel structure. Therefore, we can find that α_x approaches the curve of the parallel model and α_y shifts to the line of the series model.

The effect of the phase structure on the properties is summarized in Table II. The elastic modulus and thermal expansion coefficient after phase separation are isotropic and are defined as E_s and α_s , respectively. E_s is less than E_a , where subscript a denotes the additive rule. The change of

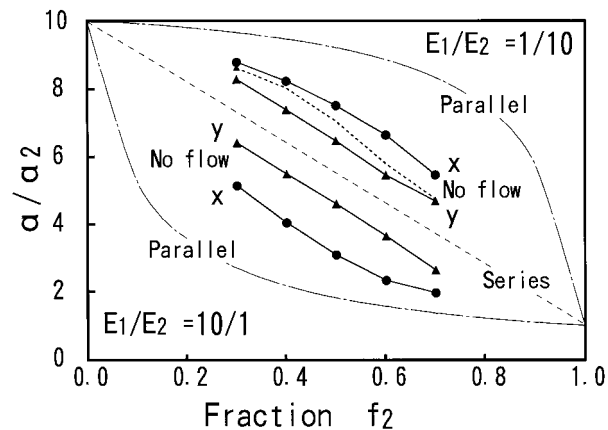


Figure 10 Effect of the shear flow on the thermal expansion coefficients.

Table II Effect of the Phase Structure on Properties

Phase separation
$E_s = E_x = E_y < E_a$ If $E_1 > E_2, \alpha_s = \alpha_x = \alpha_y < \alpha_a$ If $E_1 < E_2, \alpha_s = \alpha_x = \alpha_y > \alpha_a$
Shear flow in x direction
$E_y < E_s < E_x$ If $E_1 > E_2, \alpha_x < \alpha_s < \alpha_y$ If $E_1 < E_2, \alpha_y < \alpha_s < \alpha_x$

Subscript s denotes the additive rule and a shows properties after phase separation or initial properties before shear flow; other properties of the components are $\alpha_1 > \alpha_2$ and $\nu_1 = \nu_2$.

α_s depends on the elastic modulus of the components. If E_1 is greater than E_2 , α_s becomes less than α_a . Otherwise, α_s is greater than α_a . By applying a shear flow in the x direction, the anisotropy of the properties is caused by the structural change. E_y decreases from E_s , and E_x increases from E_s . When α_1 is greater than α_2 and if E_1 is greater than E_2 , α_x is smaller than α_s and α_y is larger than α_s ; otherwise, the tendency is inverse.

CONCLUSION

Computer programs have been developed to predict phase structures and mechanical properties for binary polymer mixtures. Structure changes due to phase separation and shear flow were investigated for various average fractions by computer simulation. The developed program could be used to reveal the effect of phase structure on the elastic modulus and thermal expansion coefficient of binary mixtures.

REFERENCES

1. J. A. Manson, *Polymer Blends and Composites*, Plenum Press, New York, 1976.
2. L. Holliday and J. Robinson, *J. Mater. Sci.*, **8**, 301 (1973).
3. J. N. Farber and R. J. Farris, *J. Appl. Polym. Sci.*, **34**, 2093 (1987).
4. S. H. Liu and E. B. Nauman, *J. Mater. Sci.*, **25**, 2071 (1990).

5. E. Sideridis and G. C. Papanicolaou, *Rheol. Acta*, **27**, 608 (1988).
6. F. J. Guild and R. J. Young, *J. Mater. Sci.*, **24**, 2454 (1989).
7. J. W. Cahn and J. E. Hilliard, *J. Chem. Phys.*, **28**, 258 (1958).
8. H. E. Cook, *Acta Metall.*, **18**, 297 (1970).
9. R. Petschek and H. Metiu, *J. Chem. Phys.*, **79**, 3443 (1983).
10. A. Chakrabarti, R. Toral, and J. Gunton, *Phys. Rev. B*, **39**, 4386 (1989).
11. M. V. Ariyapadi, E. B. Nauman, and J. W. Haus, in *Computer Simulation of Polymers*, R. J. Roe, Ed., Prentice-Hall, Englewood Cliffs, NJ, 1991, p. 374.
12. Y. Chen, K. Solc, and G. T. Caneba, *Polym. Eng. Sci.*, **33**, 1033 (1993).
13. T. Matsuoka and S. Yamamoto, *J. Appl. Polym. Sci.*, **57**, 353 (1995).